PHYSICAL REVIEW D **71,** 014026 (2005)

Strangelet propagation and cosmic ray flux

Jes Madsen

Department of Physics and Astronomy, University of Aarhus, DK-8000 Århus C, Denmark

(Received 17 November 2004; published 25 January 2005)

The galactic propagation of cosmic ray strangelets is described and the resulting flux is calculated for a wide range of parameters as a prerequisite for strangelet searches in lunar soil and with an Earth orbiting magnetic spectrometer, AMS-02. While the inherent uncertainties are large, flux predictions at a measurable level are obtained for reasonable choices of parameters if strange quark matter is absolutely stable. This allows a direct test of the strange matter hypothesis.

DOI: 10.1103/PhysRevD.71.014026 PACS numbers: 12.38.Mh, 12.39.Ba, 97.60.Jd, 98.70.Sa

I. INTRODUCTION

At densities slightly above nuclear matter density quark matter composed of up, down, and strange quarks in roughly equal numbers (called strange quark matter) may be absolutely stable, i.e., stronger bound than iron [1–4]. In spite of two decades of scrutiny, neither theoretical calculations, nor experiments or astrophysical observations have been able to settle this issue (for reviews, see [5,6]). If strange quark matter is absolutely stable it would have important consequences for models of ''neutron stars'', which would then most likely all be quark stars (strange stars [3,7–10]). It would also give rise to a significant component of strangelets (lumps of strange quark matter) in cosmic rays, and in fact the search for cosmic ray strangelets may be the most direct way of testing the stable strange matter hypothesis. A significant flux of cosmic ray strangelets could exist due to strange matter release from binary collisions of strange stars [11,12]. In the following the propagation of such cosmic ray strangelets in the Galaxy is discussed, and the resulting differential and total flux is calculated as a function of various parameters within a simple, but physically transparent propagation model. The results are of interest for the coming cosmic ray experiment on The International Space Station, Alpha Magnetic Spectrometer (AMS-02) [13–16], as well as for a lunar soil strangelet search.

II. STRANGELET PROPERTIES

Strangelets are lumps of strange quark matter with baryon number A in the possible range from a few to a few times 10^{57} (the term strangelet is sometimes used only for lumps with baryon number below $10^6 - 10^7$; here the term will be used for lumps of all A). The upper limit is the gravitational instability limit for truly macroscopic bulk quark matter in the form of strange stars. Given absolute stability of bulk strange quark matter, a lower limit on A for stable strangelets follows from the fact that surface tension and curvature energy destabilize small quark lumps relative to bulk matter. However, the stability of bulk strange quark matter as well as the value of the minimal A depends on poorly determined model parameters such as the strange quark mass, the bag constant and the strong coupling constant, so in the following, stability is simply assumed, and A is treated as a free parameter.

Several models of strange quark matter have been discussed in the literature, and it has been realized that different phases of strange quark matter may be energetically favorable depending on the values of relevant parameters. Common for all of the corresponding types of strangelets are masses per baryon below the mass of nuclei (by assumption of stability), and a very low charge-to-mass ratio compared with nuclei due to the near cancellation of up, down and strange quark charges when these quarks appear in nearly equal numbers.

In the following strangelet masses are assumed to be near the upper limit for stability,

$$mc^2 = m_0 c^2 A \approx 0.93 \text{ GeV} A. \quad (1)$$

Slightly lower masses are possible, and the assumption made here neglects the fact that the strangelet mass per baryon decreases slightly with A in model calculations. These effects are of negligible consequence relative to the far larger uncertainties in other parameter choices below.

Strangelet charges, Z, are significantly lower than the $Z \approx A/2$ known from nuclei, and this is the most important experimental signature for strangelet detection. For the sake of example, most results in the figures below assume strangelets to be color-flavor locked with a charge [17]

$$Z = 0.3A^{2/3}. \quad (2)$$

This assumes a strange quark mass of 150 MeV (the charge of color-flavor locked strangelets is proportional to the strange quark mass [17]). Color-flavor locked quark matter is electrically neutral in bulk [18], because the pairing of quarks is optimized when all three quark flavors have equal Fermi momenta and thereby equal bulk number densities. However, a depletion of massive strange quarks at the surface of a finite quark matter lump leads to a net positive charge proportional to the surface area or $A^{2/3}$ [17,19]. Strangelets without pairing (''ordinary'' strangelets) have charge [20]

$$Z = 0.1A \quad (3)$$

$$Z = 8A^{1/3} \quad (4)$$

for $A \ll 700$ and $A \gg 700$ respectively, again assuming a strange quark mass of 150 MeV (here the charge is proportional to m_s^2 [4,20,21]).

Strangelets may be neutralized by electrons and form unusual ions or atoms. At very high charges ($Z \gg 10^2$), the strangelets are automatically partly neutralized by electrons from the excitation of the vacuum [22], so the net charge increases slower with mass than indicated in the relations above. For most of the results below the masses are below the range where such effects become important. Also, for most of the calculations the cosmic ray strangelets have energies where full ionization is a good approximation, but the effective charge is smaller than Z at small velocities, c.f. Eq. (15) below.

III. STRANGELET PRODUCTION

The production of strangelets is speculative, but could happen when two strange stars in a binary system spiral towards each other due to loss of orbital energy in the form of gravitational radiation. If strange quark matter is absolutely stable (the assumption in this paper for stable cosmic ray strangelets to exist) all compact stars are likely to be strange stars [11,12], and therefore the galactic coalescence rate will be the one for double neutron star binaries recently updated in [23] based on available observations of binary pulsars to be $83.0^{+209.1}_{-66.1}$ Myr^{-1} at a 95% confidence interval, thus of order one collision in our Galaxy every 3000–60 000 years.

Each of these events involve a phase of tidal disruption of the stars as they approach each other before the final collision. During this stage small fractions of the total mass may be released from the binary system in the form of strange quark matter. No realistic simulation of such a collision involving two strange stars has been performed to date. Newtonian and semirelativistic simulations of the inspiral of strange stars and black holes do exist [24–26], but the physics is too different from the strange star-strange star collision to be of guidance. Simulations of binary neutron star collisions, depending on orbital and other parameters, lead to the release of anywhere from $10^{-5} - 10^{-2} M_\odot$, where $M_\odot$ denotes the solar mass, corresponding to a total mass release in the Galaxy of anywhere from $10^{-10} - 3 \times 10^{-6} M_\odot$ per year with the collision rate above. Given the high stiffness of the equation of state for strange quark matter, strange star-strange star collisions should probably be expected to lie in the low end of the mass release range, so the canonical input for the following calculations is a galactic production rate of

$$\dot{M} = 10^{-10} M_\odot \text{ yr}^{-1}. \quad (5)$$

All strangelets released are assumed to have a single baryon number, A. This is clearly a huge oversimplification, but there is no way of calculating the actual mass spectrum to be expected. As demonstrated in [16] the quark matter lumps originally released by tidal forces are macroscopic in size (when estimated from a balance between quark matter surface tension and tidal forces), but subsequent collisions will lead to fragmentation, and under the assumption that the collision energy is mainly used to compensate for the extra surface energy involved in making smaller strangelets, it was argued that a significant fraction of the mass released from binary strange star collisions might ultimately be in the form of strangelets with $A \approx 10^2 - 10^4$, though these values are strongly parameter dependent.

Fortunately, most of the total flux results derived for cosmic ray strangelets below are such that values for some given A are valid as a lower limit for the flux for a fixed total strangelet mass injection if strangelets are actually distributed with baryon numbers below A.

IV. STRANGELETS IN COSMIC RAYS: ACCELERATION AND PROPAGATION

Apart from an unusually high A/Z-ratio compared to nuclei, strangelets would in many ways behave like ordinary cosmic ray nuclei. For example, the most likely acceleration mechanism would be Fermi acceleration in supernova shocks resulting in a rigidity spectrum at the source which is a powerlaw in rigidity as described below. Because of the high strangelet rigidity, R, at fixed velocity ($R \equiv pc/Ze = Am_0c^2\gamma(\beta)\beta/Ze$, where p is the strangelet momentum, $\beta \equiv v/c$, and $\gamma = (1 - \beta^2)^{-1/2}$) strangelets are more efficiently injected into an accelerating shock than are nuclei with $A/Z \approx 2$ (c.f. discussion of nuclei in [27]), and one may expect that most strangelets passed by a supernova shock will take part in Fermi acceleration.

The time scales for strangelet acceleration, energy loss, spallation and escape from the Galaxy are all short compared to the age of the Milky Way Galaxy. This makes it reasonable to assume that cosmic ray strangelets are described by a steady state distribution, i.e., as a solution to a propagation equation of the form

$$\frac{dN}{dt} = 0 \quad (6)$$

where $N(E, x, t)dE$ is the number density of strangelets at position x and time t with energy in the range $[E, E + dE]$. In standard form (e.g., [28,29]; given the significant uncertainty in input parameters in the present investigation, a simple but physically transparent model for strangelet propagation is chosen) $\frac{dN}{dt}$ is given by the following sum of a source term from supernova acceleration, a diffusion term, loss terms due to escape from the Galaxy, energy loss, decay, spallation, and a term to describe reacceleration of strangelets due to passage of new supernova shock waves,

$$\frac{dN}{dt} = \frac{\partial N}{\partial t}|_{\text{source}} + D\nabla^2 N + \frac{\partial N}{\partial t}|_{\text{escape}} + \frac{\partial}{\partial E}[b(E)N] + \frac{\partial N}{\partial t}|_{\text{decay}} + \frac{\partial N}{\partial t}|_{\text{spallation}} + \frac{\partial N}{\partial t}|_{\text{reacceleration}}. \quad (7)$$

The individual terms will be defined and discussed in the following subsections.

A. Source term

The strangelet spectrum after acceleration in supernova shocks is assumed to be a standard powerlaw in rigidity as derived from observations of ordinary cosmic rays,

$$g(R) = \frac{\alpha - 1}{R_{\text{min}}^{1-\alpha} - R_{\text{max}}^{1-\alpha}} R^{-\alpha}, \quad (8)$$

where rigidity R is measured in GV, powerlaw index $\alpha \approx 2.2$, and the normalization is such that $\int_{R_{\text{min}}}^{R_{\text{max}}} g(R)dR = 1$. The minimal rigidity is assumed to be given by the speed of a typical supernova shock wave, $\beta_{SN} \approx 0.005$, where $v \equiv \beta c$ is the speed, so $R_{\text{min}} = \gamma(\beta_{SN})\beta_{SN} A m_0 c^2/Ze \approx 5\ \text{MV}A/Z$. The maximal rigidity from acceleration in supernova shocks, R_{max}, is of order 10^6 GV, but the actual number is irrelevant since $R_{\text{max}} \gg R_{\text{min}}$ and $g(R)$ decreases rapidly with increasing R.

The source term is normalized according to a total production rate of $\dot{M} = 10^{-10} M_\odot\ \text{yr}^{-1}$ of baryon number A strangelets spread evenly in an effective galactic volume (see the following subsection) of $V = 1000\ \text{kpc}^3$, giving a total source term

$$G(R) = \frac{\dot{M}}{VAm_0} g(R) \quad (9)$$

or in terms of energy (using $dE/dR = Ze\beta$ and $G(R)dR = G(E)dE$)

$$\frac{\partial N}{\partial t}|_{\text{source}} \equiv G(E) = \frac{G[R(E)]}{Ze\beta}. \quad (10)$$

B. Spatial diffusion and escape

The terms $D\nabla^2 N + \frac{\partial N}{\partial t}|_{\text{escape}}$, where D is the diffusion coefficient, describe cosmic ray diffusion in real space and eventual escape from the confining magnetic field of the Galaxy. Charged cosmic rays are spiralling along field lines in the weak galactic magnetic field, but due to the very irregular structure of the field, the particles scatter on magnetic ''impurities'', and the motion is best described in terms of diffusion. From studies of nuclei, it is known that cosmic rays are confined to move in a region significantly larger than the galactic disk, where most of the stars and interstellar matter are located. A typical value for the effective galactic volume confining cosmic rays is $V = 1000\ \text{kpc}^3$ as chosen above. We will make a standard leaky box approximation, assuming $D = 0$ and $\frac{\partial N}{\partial t}|_{\text{escape}} = -N/\tau_{\text{escape}}$, where $\tau_{\text{escape}}(A, Z, E)$ is the average escape time from an otherwise homogeneous distribution in the galactic volume, V. From studies of cosmic ray nuclei the average column density of material, ξ_{escape}, passed by nuclei before escape from the Galaxy is known as a function of rigidity, R, as

$$\xi_{\text{escape}} = \xi_0 \left(\frac{R}{R_0}\right)^{\delta}, \quad (11)$$

where $\xi_0 = 12.8\ \text{g/cm}^2$, $R_0 = 4.7$ GV, $\delta = 0.8$ for $R < R_0$, and $\delta = -0.6$ for $R > R_0$. Strangelets are sufficiently similar to nuclei for the same distribution of column density to be assumed. The corresponding time scale is given by $\tau = \xi/(\rho v)$, where ρ is the density of the interstellar medium (largely atomic and molecular hydrogen). With n denoting the average hydrogen number density per cubic centimeter ($n \approx 0.5$ when averaging over denser regions in the galactic plane and dilute regions in the magnetic halo), the resulting escape time scale for strangelets is

$$\tau_{\text{escape}} = \frac{8.09 \times 10^6\ \text{y}}{n\beta} \left(\frac{R}{R_0}\right)^{\delta}. \quad (12)$$

C. Energy loss

The term in the propagation equation $\frac{\partial}{\partial E}[b(E)N]$, describes the influence of energy loss processes. The energy loss rate $b(E) \equiv -dE/dt$ can be treated as a sum of ionization losses (from interaction with neutral hydrogen atoms and molecules), Coulomb losses (from interaction with ionized hydrogen), and pion production losses from inelastic collisions at high relativistic γ-factor (threshold at $\gamma = 1.3$). Since Coulomb losses are generally negligible compared to the other two mechanisms, only ionization and pion production will be considered.

1. Pion production loss

In accordance with the relations for nuclei given in [30] we assume

$$\frac{dE}{dt}|_{\text{pion}} = -1.82 \times 10^{-7} n A^{0.53} 0.72 \gamma^{1.28} H(\gamma - 1.3)\ \text{eV/s}, \quad (13)$$

where H is the Heaviside step function taking account of the pion production threshold, and the Lorentz-factor is $\gamma = (1 - \beta^2)^{-1/2}$.

2. Ionization loss

The energy loss due to ionization is given by [30]

$$\frac{dE}{dt}|_{\text{ionization}} = -1.82 \times 10^{-7} n Y(Z, \beta)^2 [1 + 0.0185 \ln(\beta) H(\beta - 0.01)] \times \frac{2\beta^2}{10^{-6} + 2\beta^3}\ \text{eV/s}, \quad (14)$$

where the effective charge Y is smaller than Z at small velocities as described by

$$Y(Z, \beta) = Z[1 - 1.034 \exp(-137\beta Z^{-0.688})]. \quad (15)$$

This relation is based on fits to intermediate and high-Z nuclei, and it is not expected to work at very low values of β. However it is sufficient for the present purpose since the strangelet cosmic ray spectrum at the lowest energies is dramatically reduced by solar modulation anyway. At speeds close to the speed of light the ionization loss is simply proportional to nZ^2.

D. Decay

The existence of a measurable cosmic ray strangelet flux requires strangelets to be stable. Thus, it is assumed that $\frac{\partial N}{\partial t}|_{\text{decay}} = 0$.

E. Spallation

Like nuclei, strangelets have a roughly geometrical cross section (proportional to $A^{2/3}$) for spallation in collisions with interstellar matter (hydrogen). The corresponding spallation time scale is taken to be

$$\tau_{\text{spallation}} = \frac{2 \times 10^7 \text{y}}{n\beta} A^{-2/3}, \quad (16)$$

where the normalization comes from data for nuclei at kinetic energy above 2 GeV. At low kinetic energy the cross section for nuclei (and presumably strangelets) can vary somewhat due to resonances etc, but such complications will be neglected here, since the detailed physics is unknown in the case of strangelets. We have also neglected the slight reduction in geometrical area of strangelets relative to nuclei due to their slightly larger density. The largest uncertainty in the treatment of spallation is the fact that strangelets (like nuclei) are not always completely destroyed in a spallation reaction. In addition to nucleons and nuclei, smaller strangelets may result from this type of reaction, but we are ignorant of the physics to an extent where it is impossible to include this effective feed-down to lower A in a meaningful manner. Therefore, spallation is assumed to be a process destroying strangelets, i.e.,

$$\frac{\partial N}{\partial t}|_{\text{spallation}} = -\frac{N}{\tau_{\text{spallation}}}. \quad (17)$$

This leads to an overall underestimate of the strangelet flux.

F. Reacceleration

Strangelet energies are redistributed according to the propagation equation. Some leave the Galaxy or are destroyed by spallation. Occasionally strangelets get a new kick from a passing supernova shock, and in a first approximation they regain the source term relative distribution of rigidity, $g(R)$. The time scale between supernova shock waves passing a given position in interstellar space is of order $\tau_{SN} \approx 10^7$ y. This scale is comparable to or larger than the time scales for energy loss, spallation, and escape from the Galaxy, so reacceleration of cosmic ray strangelets has only a moderate influence on the steady state distribution. By adding energy (on average) to the particles it actually reduces the total flux of strangelets somewhat because higher energies make destruction and escape more likely. The reacceleration mechanism has been taken into account by adding terms to the right hand side of the propagation equation of the form

$$\frac{\partial N}{\partial t}|_{\text{reacceleration}} = -\frac{N}{\tau_{SN}} + \frac{\int N(E)dE}{\tau_{SN}} g(R) \frac{dR}{dE}, \quad (18)$$

where the first term describes how particles are taken out of the spectrum on a time scale τ_{SN}, and the second term reintroduces these particles with the source term rigidity power law distribution.

The importance of reacceleration relative to the source term from new strangelets is parametrized by K, which is given as

$$K = \left[\frac{\int N(E)dE}{\tau_{SN}}\right] \Big/ \left[\frac{\dot{M}}{VAm_0}\right]. \quad (19)$$

Because of the large value of τ_{SN} (of order 10^7 years, which is comparable to or bigger than the other relevant time scales), K is typically rather small, and therefore reacceleration plays a minor role (factor of 2 or less for typical parameters).

G. The energy distribution

Introducing the terms discussed above the steady state equation $\frac{dN}{dt} = 0$ leads to the following differential equation for $N(E)$

$$b(E) \frac{dN}{dE} = \frac{N(E)}{\tau(E, A, Z)} - [1 + K]G(E), \quad (20)$$

where

$$1/\tau(E, A, Z) = 1/\tau_{\text{escape}} + 1/\tau_{\text{spallation}} + 1/\tau_{SN} + 1/\tau_{\text{loss}}, \quad (21)$$

with $1/\tau_{\text{loss}} \equiv -db(E)/dE$.

H. The interstellar flux

Given a solution for $N(E)$ the corresponding flux in the "average" interstellar medium with energies from $[E, E + dE]$ is given by

$$F_E(E)dE = \frac{\beta c}{4\pi} N(E)dE, \quad (22)$$

and the corresponding flux in terms of rigidity is

$$F_R(R)dR = Ze\beta F_E[E(R)]dR \quad (23)$$

(using $dE/dR = Ze\beta$).

I. Solar modulation

Like other charged cosmic ray particles strangelets are influenced by the solar wind when entering the inner parts of the Solar System. The detailed interactions are complicated, but as demonstrated for nuclei in [31], a good fit to the solar modulation of the cosmic ray spectrum can be given in terms of a potential model, where the charged particle climbs an electrostatic potential of order $\Phi = 500$ MeV (the value changes by a factor of less than 2 during the 11 (22) year solar cycle). This effectively reduces the cosmic ray energy by $|Z|\Phi$ relative to the value in interstellar space, and at the same time the flux is reduced by the relative reduction in particle momentum squared, so that the modulated spectrum is

$$F_{\rm mod}(E) = \left(\frac{R(E)}{R(E + |Z|\Phi)}\right)^2 F_E(E + |Z|\Phi). \qquad (24)$$

Solar modulation significantly suppresses the flux of charged cosmic rays at energies below a few GeV. The solar modulation effectively works like a smooth cutoff in flux below kinetic energy of order $Z\Phi$. Since strangelets have a high mass-to-charge ratio they are nonrelativistic at these energies, which correspond to rigidities in GV of $R_{\rm GV} \approx (A/Z)^{1/2}\Phi_{500}^{1/2}$, where $\Phi_{500} = \Phi/(500\ {\rm MeV})$.

J. Geomagnetic cutoff

For cosmic rays to reach the Earth or an Earth-orbiting detector like the Alpha Magnetic Spectrometer on the International Space Station, the energies have to exceed the geomagnetic cutoff rigidity, which is a function of detector position, and for an orbiting observatory like AMS the value varies from 1–15 GV as a function of time. Notice that the geomagnetic cutoff rigidity for low mass strangelets is comparable to or higher than the solar modulation cutoff, whereas high mass strangelets experience solar modulation already at rigidities above the geomagnetic cutoff.

For a nonmagnetic body like the Moon, there is no corresponding cutoff, and the total flux is given by $F_{\rm mod}$.

V. RESULTS

A. Special cases

While the general solution of the propagation equation requires numerical integration, several limits can be treated analytically and provide a physical understanding of the full numerical solutions that follow below. The special cases (disregarding solar modulation and geomagnetic cutoff) can be divided according to the relative importance of the different time scales, $\tau_{\rm escape}$, $\tau_{\rm spallation}$, τ_{SN} and $\tau_{\rm loss}$ (or rather $|\tau_{\rm loss}|$, since the energy loss time scale as defined above is negative at low and high energies, describing a net increase in number of particles).

When one of the time scales is significantly smaller than the others at a given energy (rigidity), the corresponding process dominates the physics. The relative importance of the processes depends on strangelet properties A, Z, on the density of interstellar hydrogen n (though most processes have the same n-dependence), and of course on the strangelet energy, E (or equivalently rigidity, R, speed, β, or Lorentz-factor, γ). For most strangelet masses and charges, τ_{SN} is larger than one or more of the other time scales. Typically, energy loss dominates at low-energy, spallation at intermediate E, and escape from the Galaxy at the highest energies. Figure 1 compares the different time scales for color-flavor locked strangelets with $Z = 8, A \approx 138$. The energy loss time scale plotted is $|\tau_{\rm loss}|$, whereas $\tau_{\rm loss}$ itself is negative to the right and left of the parabolalike section of $|\tau_{\rm loss}|$ between rigidities of order 0.5 to 10 GV. The total time scale is negative below 0.5 GV, since it is almost equal to the energy loss time scale in this regime.

1. Low-energy; energy loss domination

At low energies $\tau \approx \tau_{\rm loss}$, and the propagation equation reduces to

$$\frac{d}{dE}[b(E)N(E)] \approx -G(E), \qquad (25)$$

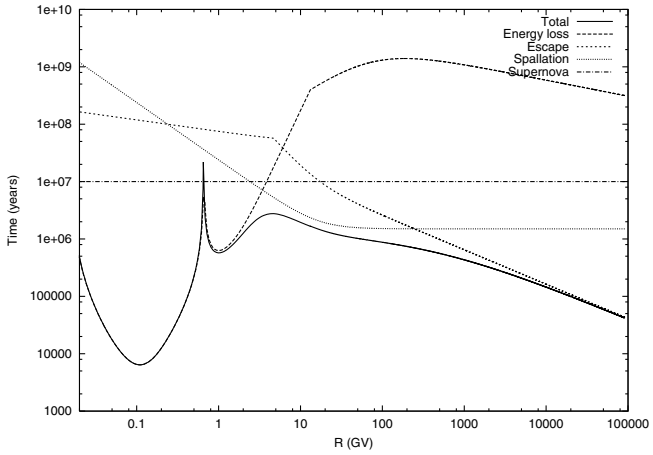

FIG. 1. Characteristic time scales (in years) as a function of rigidity (in GV) for the processes dominating the propagation of strangelets: Energy loss ($|\tau_{\rm loss}|$; long-dashed), escape from the Galaxy ($\tau_{\rm escape}$; short-dashed), spallation ($\tau_{\rm spallation}$; dotted), and reacceleration in supernova shocks (τ_{SN}; dotted-dashed). The total time scale, τ, is shown by the solid curve. All time scales are shown positive, but $\tau_{\rm loss}$ is actually negative outside the parabolalike regime from 0.5–10 GV (it becomes positive again at very low values of R). The total time scale is dominated by energy loss below approximately 3 GV and follows the sign change of $\tau_{\rm loss}$ there. For intermediate rigidities spallation is most important, and at high R escape from the Galaxy is the fastest and therefore dominating process. The example given assumes color-flavor locked strangelets with $Z = 8$ ($A \approx 138$) and neglects solar modulation and geomagnetic cutoff.

which can be integrated to give

$$N(E) \approx -\frac{\int_{\infty}^{E} G(E')dE'}{b(E)}. \quad (26)$$

At the very lowest energies for which the source term $g(R) = 0$ (this happens when $R < R_{\rm min}$), the integral in the numerator is a (negative) constant, and $N(E) \propto 1/b(E)$. Above $R_{\rm min}$, $N(E) \propto (R/R_{\rm min})^{-1.2}/b(E)$. The corresponding flux in terms of rigidity includes an additional β^2-dependence proportional to R^2 in the nonrelativistic domain. In this domain energy loss by ionization dominates. If the strangelet charge were constant, the flux would be constant at very low R, followed by regimes with decreasing flux proportional to $R^{-1.2}$, increasing flux proportional to $R^{1.8}$, and another regime with the flux decreasing like $R^{-1.2}$ when approaching the realm of relativistic strangelets (however, except for very low (A, Z), the energy loss domination is only relevant for nonrelativistic strangelets).

Figure 2 shows the differential flux as a function of rigidity for $Z = 8, A \approx 138$ (as in Fig. 1). The low energy domain of the full numerical solution (marked ''Interstellar flux'') shows a decrease rather than constant flux at the far left end, followed by a slightly steeper decrease for $R > R_{\rm min}$, an increase, and again a decrease in flux. In general, the flux is higher at low R and the decrease with R steeper (increase with R less steep) than would be expected from the arguments above. This is because the effective charge

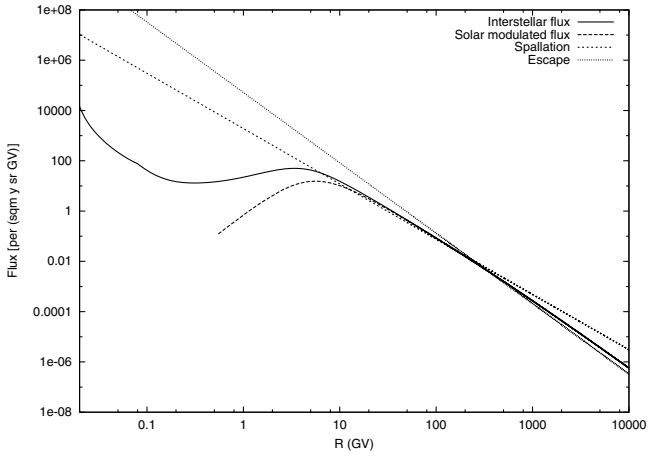

FIG. 2. The differential strangelet flux as a function of rigidity assuming color-flavor locked strangelets with $Z = 8, A \approx 138$. The solid curve shows the ''interstellar flux'', i.e., the average flux in the Galaxy without inclusion of solar modulation and geomagnetic cutoff. The long-dashed curve includes solar modulation. Geomagnetic cutoff may eliminate the flux below rigidities of a few GV for a detector in Earth orbit, whereas no such effect exists for strangelets hitting the Moon or other nonmagnetic objects. Short-dashed and dotted curves show the effects of spallation and galactic escape domination, respectively. It is seen that these processes explain the behavior in specific rigidity regimes, as discussed in the text.

$Y(Z, \beta)$ is less than Z for nonrelativistic strangelets and approaches 0 for low R. (In fact, the effective charge as defined here becomes negative at finite R. This is of course unphysical, but reflects the fact that the energy loss due to ionization becomes negligible).

2. Intermediate energy; spallation domination

At intermediate and high energies energy loss processes can be neglected, and thus $b(E) \approx 0$, corresponding to $|\tau_{\rm loss}| \approx \infty$. For most parameter choices this shift takes place at rigidities somewhat below the solar modulation cutoff discussed above. At intermediate energies the spectrum is determined by the strangelet spallation time, $\tau \approx \tau_{\rm spallation}$, and the propagation equation is approximately given by

$$N(E) \approx [1 + K]G(E)\tau_{\rm spallation}(n, \beta, A) \quad (27)$$

with $\tau_{\rm spallation} = 2 \times 10^7 {\rm y} n^{-1} \beta^{-1} A^{-2/3}$.

Assuming also $K = 0$ (equivalent to $\tau_{\rm SN} \gg \tau_{\rm spallation}$) gives the approximate result

$$F_R(R) = 2.34 \times 10^5 \ {\rm m}^{-2} \ {\rm yr}^{-1} \ {\rm sterad}^{-1} \ {\rm GV}^{-1} A^{-0.467} \times Z^{-1.2} R_{\rm GV}^{-2.2} \Lambda, \quad (28)$$

or for the total flux above rigidity R

$$F(>R) = 1.95 \times 10^5 \ {\rm m}^{-2} \ {\rm yr}^{-1} \ {\rm sterad}^{-1} \ A^{-0.467} Z^{-1.2} R_{\rm GV}^{-1.2} \Lambda. \quad (29)$$

In both cases the results are proportional to

$$\Lambda = \left(\frac{\beta_{\rm SN}}{0.005}\right)^{1.2} \left(\frac{0.5 \ {\rm cm}^{-3}}{n}\right) \left(\frac{\dot{M}}{10^{-10} M_\odot \ {\rm yr}^{-1}}\right) \times \left(\frac{1000 \ {\rm kpc}^3}{V}\right) \left(\frac{930 \ {\rm MeV}}{m_0 c^2}\right). \quad (30)$$

Notice that the differential strangelet spectrum keeps the source term slope, $G(R) \propto R^{-2.2}$. This is also clearly seen in Fig. 2, where the spallation regime corresponds to rigidities from a few GV to a few tens of GV. Figure 3 shows the corresponding curves for the integrated flux $(F(>R))$.

3. High energy; escape time domination

The intermediate energy domain is replaced by the high energy domain when $\tau_{\rm escape} \leq \tau_{\rm spallation}$. Except for very low A this happens when $R > R_0[2.5A^{-2/3}]^{-1/0.6} \approx 1.0 \ {\rm GV} A^{1.11}$, or $E > 1.0 \ {\rm GeV} Z A^{1.11} \beta^{-1}$. At high energies the spectrum is determined by the confinement time of strangelets in the Galaxy, $\tau \approx \tau_{\rm escape}$, and the propagation equation is approximately given by

$$N(E) \approx G(E)\tau_{\rm escape}(n, \beta, R). \quad (31)$$

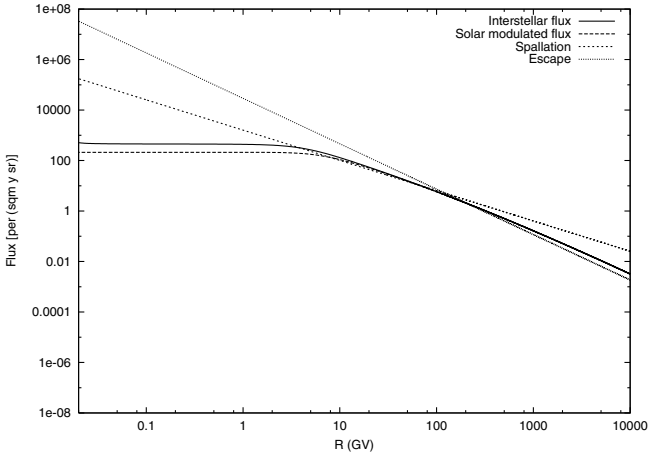

FIG. 3. The integrated strangelet flux at rigidity higher than R. Parameters and curves as in Fig. 2.

For semirelativistic or relativistic strangelets with $\beta \approx 1$, $\tau_{\rm escape} \propto R^{-0.6}$, so the spectrum is steepened from the source term $R^{-2.2}$ to $R^{-2.8}$.

Again assuming $K = 0$ (equivalent to $\tau_{\rm SN} \gg \tau_{\rm escape}$) gives the approximate result

$$F_R(R) = 2.40 \times 10^5 \text{ m}^{-2} \text{ yr}^{-1} \text{ sterad}^{-1} \text{ GV}^{-1} A^{0.2} \times Z^{-1.2} R_{\rm GV}^{-2.8} \Lambda, \quad (32)$$

and for the total flux above rigidity R

$$F(>R) = 1.33 \times 10^5 \text{ m}^{-2} \text{ yr}^{-1} \text{ sterad}^{-1} A^{0.2} Z^{-1.2} R_{\rm GV}^{-1.8} \Lambda. \quad (33)$$

Comparison with Figs. 2 and 3 shows good agreement at high R (the small difference is due to reacceleration).

4. Rule of thumb for the total flux

Since the astrophysical input parameters in the present calculations are uncertain at the order of magnitude level, relations for the total flux of strangelets hitting the Earth or Moon accurate within a factor of 2 (for fixed input parameters) are useful. As indicated above solar modulation effectively cuts off the strangelet flux at rigidities of order $R_{\rm SM} \approx (A/Z)^{1/2} \Phi_{500}^{1/2}$ GV, which is in the part of the spectrum where the strangelet flux is governed by spallation. The total flux hitting the Moon or Earth is therefore roughly given by

$$F_{\rm total} \approx 2 \times 10^5 \text{ m}^{-2} \text{ yr}^{-1} \text{ sterad}^{-1} A^{-0.467} Z^{-1.2} \times \max[R_{\rm SM}, R_{\rm GC}]^{-1.2} \Lambda, \quad (34)$$

depending on whether solar modulation or geomagnetic cutoff dominates. In the case of solar modulation domination (always relevant for the Moon, and relevant for AMS as long as $R_{\rm SM} > R_{\rm GC}$) one obtains

$$F_{\rm total} \approx 2 \times 10^5 \text{ m}^{-2} \text{ yr}^{-1} \text{ sterad}^{-1} A^{-1.067} Z^{-0.6} \Phi_{500}^{-0.6} \Lambda. \quad (35)$$

For strangelets obeying the CFL mass-charge relation $Z = 0.3A^{2/3}$ this becomes

$$F_{\rm total} \approx 4 \times 10^5 \text{ m}^{-2} \text{ yr}^{-1} \text{ sterad}^{-1} A^{-1.467} \Phi_{500}^{-0.6} \Lambda \quad (36)$$

$$\approx 2.8 \times 10^4 \text{ m}^{-2} \text{ yr}^{-1} \text{ sterad}^{-1} Z^{-2.2} \Phi_{500}^{-0.6} \Lambda, \quad (37)$$

which reproduces the numerical results to within 20% for $Z > 10$ and to within a factor of a few even for small Z, where the assumptions of nonrelativistic strangelets and spallation domination both are at the limit of being valid.

B. Numerical results

Figs. 2 and 3 show the interstellar strangelet fluxes as a function of rigidity, as well as the fluxes reduced by solar modulation. Differential fluxes as well as integrated fluxes are displayed for strangelets with charge $Z = 8$, and baryon number $A \approx 138$ given by the charge-mass relation for color-flavor locked strangelets.

Figs. 4 and 5 show the total strangelet flux as a function of strangelet charge and baryon number, respectively, assuming the CFL-relation for the charge. Figs. 6 and 7 show similar results, assuming the charge-mass relation of ''ordinary'' strangelets. Figs. 4–7 do not include geomagnetic cutoff, so they are relevant for the Moon, whereas fluxes could be reduced for a detector in Earth orbit, depending primarily on geomagnetic latitude. Notice the nice agreement between the numerical calculations and the approximation to $F_{\rm total}$ given above, except at very low charge.

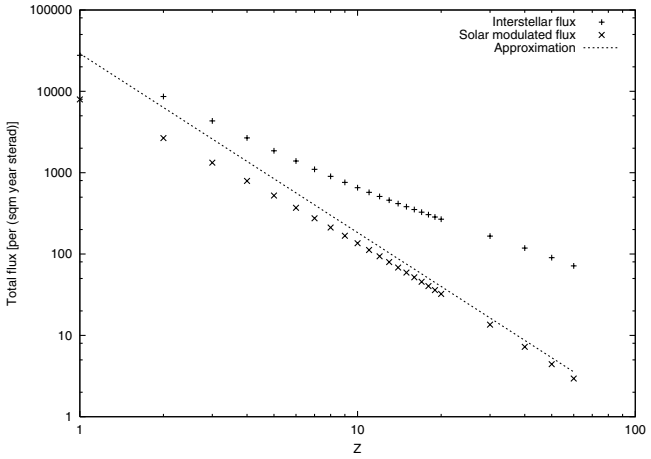

FIG. 4. The total strangelet flux as a function of charge for interstellar conditions and near Earth taking account of solar modulation, but not geomagnetic cutoff. The approximation in Eq. (35) is seen to reproduce the local strangelet flux very well, except at very low Z. Strangelets are assumed to follow the CFL charge-mass relation.

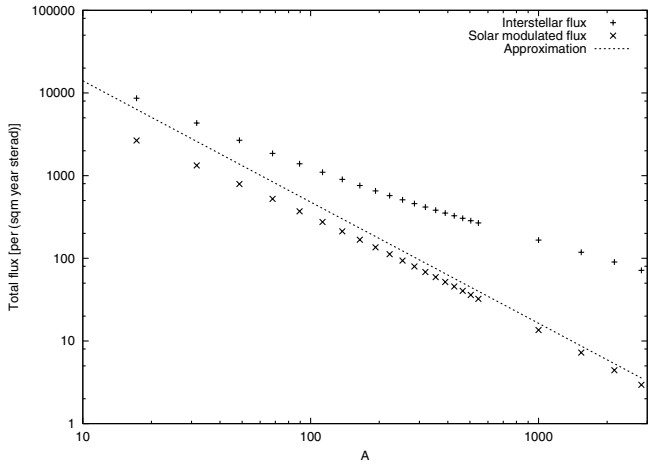

FIG. 5. As Fig. 4, except that the total flux is now shown as a function of baryon number.

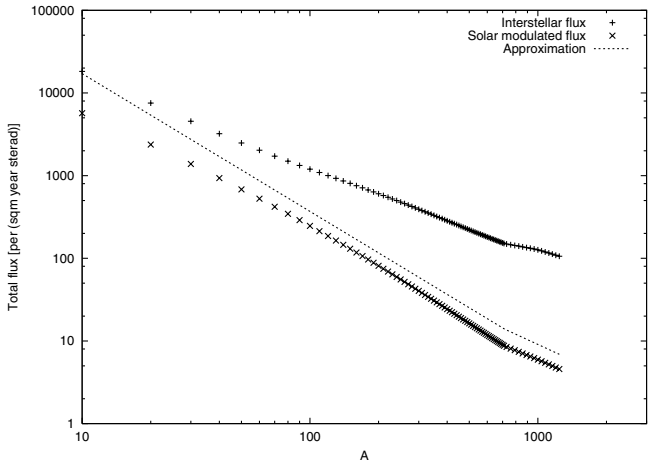

FIG. 7. As Fig. 6, except that the flux of ordinary strangelets is shown as a function of baryon number.

The strangelet flux calculated for Λ of order unity is high enough to be of interest for various upcoming experimental searches, and at the same time small enough to agree with previous searches which have given upper limits or shown marginal evidence for signatures consistent with strangelets (see [15] for an overview). As stressed several times above, many parameters are uncertain at the order of magnitude level. The scaling with these parameters is indicated where relevant. In particular this is true for the overall normalization of the strangelet flux as expressed via the parameter Λ (Eq. (30)), whereas the relative behavior of the differential flux is less uncertain.

Apart from the uncertainty in parameters within the picture discussed here, one cannot rule out the possibility that some of the basic assumptions need to be modified. In addition to strangelet production in strange star collisions, it has been suggested that a (possibly small) flux of strangelets may be a direct outcome of the Type II supernova explosions [32], where strange stars form. A detailed quantitative treatment of this mechanism for cosmic ray strangelet production does not exist. The treatment in the present paper does not include such additional strangelet production mechanisms, and therefore the flux predictions are conservative. Another assumption that leads to a conservative lower limit on the flux is that spallation is assumed to destroy strangelets completely. At least for low-energy collisions one would expect that fragments of strangelets would survive, but the input physics for performing a realistic strangelet spallation study is not sufficiently well known, and therefore the conservative assumption of complete destruction was made in the present study. A numerical simulation of strangelet propagation in Ref. [33] assumed stripping of nucleons rather than complete destruction of strangelets in interstellar collisions and studied two specific examples for the mass and energy of strangelets injected into the interstellar medium. Several other assumptions made in that numerical study differ from those of the current investigation, and therefore a direct comparison of the results is not possible, except for the reassuring fact that both studies are consistent with the possibility of a significant, measurable strangelet flux in our part of the Galaxy.

But ultimately the question of whether strangelets exist in cosmic rays is an experimental issue.

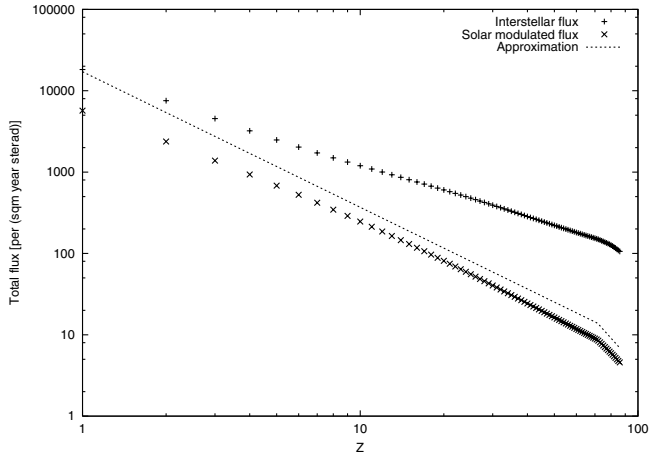

FIG. 6. As Fig. 4, except that the charge-mass relation for ordinary strangelets rather than color-flavor locked strangelets is assumed. The change in slope near $Z = 70$ is due to the change in slope of the Z-A relation for ordinary strangelets.

VI. CONCLUSION

Strangelet fluxes have been calculated numerically and compared to approximate values derived in various parameter regimes. The total strangelet flux reaching the Moon or a detector in Earth orbit is in a regime that could be within experimental reach, and therefore provide a crucial test of the hypothesis of absolutely stable strange quark matter.

ACKNOWLEDGMENTS

This work was supported by the Danish Natural Science Research Council. I appreciate the hospitality of DOE's Institute for Nuclear Theory in Seattle, where part of this work was carried out. I thank Alexei Chikanian, Evan Finch, Richard Majka, and Jack Sandweiss for comments and suggestions, and Jonas Møller Larsen for joint efforts in an early phase of this work.

[1] A. R. Bodmer, Phys. Rev. D **4**, 1601 (1971).
[2] S. A. Chin and A. K. Kerman, Phys. Rev. Lett. **43**, 1292 (1979).
[3] E. Witten, Phys. Rev. D **30**, 272 (1984).
[4] E. Farhi and R. L. Jaffe, Phys. Rev. D **30**, 2379 (1984).
[5] F. Weber, Prog. Part. Nucl. Phys. **54**, 193 (2005).
[6] J. Madsen, Lect. Notes Phys. **516**, 162 (1999).
[7] P. Haensel, J. L. Zdunik, and R. Schaeffer, Astron. Astrophys. **160**, 121 (1986).
[8] C. Alcock, E. Farhi, and A. Olinto, Astrophys. J. **310**, 261 (1986).
[9] N. K. Glendenning, in *Compact stars: Nuclear physics, particle physics, and general relativity* (Springer, New York 2000), 2nd edition.
[10] F. Weber, in *Pulsars as astrophysical laboratories for nuclear and particle physics* (IOP Publishing, Bristol, 1999).
[11] J. Madsen, Phys. Rev. Lett. **61**, 2909 (1988).
[12] J. L. Friedman and R. R. Caldwell, Phys. Lett. B **264**, 143 (1991).
[13] AMS Collaboration, M. Aguilar *et al.*, Phys. Rep. **366**, 331 (2002);**380**, 97(E) (2003).
[14] AMS Collaboration, C. H. Chung *et al.* (to be published).
[15] J. Sandweiss, J. Phys. G **30**, S51 (2004).
[16] J. Madsen, J. Phys. G **28**, 1737 (2002).
[17] J. Madsen, Phys. Rev. Lett. **87**, 172003 (2001).
[18] K. Rajagopal and F. Wilczek, Phys. Rev. Lett. **86**, 3492 (2001).
[19] J. Madsen, Phys. Rev. Lett. **85**, 4687 (2000).
[20] H. Heiselberg, Phys. Rev. D **48**, 1418 (1993).
[21] M. S. Berger and R. L. Jaffe, Phys. Rev. C **35**, 213 (1987).
[22] J. Madsen and J. M. Larsen, Phys. Rev. Lett. **90**, 121102 (2003).
[23] V. Kalogera *et al.*, Astrophys. J. **601**, L179 (2004).
[24] W. H. Lee, W. Kluzniak, and J. Nix, Acta Astronomica **51**, 331 (2001).
[25] W. Kluzniak and W. H. Lee, Mon. Not. R. Astron. Soc. **335**, L29 (2002).
[26] M. Prakash and J. M. Lattimer, J. Phys. G **30**, S451 (2004).
[27] U. D. J. Gieseler, T. W. Jones, and H. Kang, Astron. Astrophys. **364**, 911 (2000).
[28] M. S. Longair, in *High-energy astrophysics. Vol. 2: Stars, the galaxy and the interstellar medium* (Cambridge University Press, Cambridge, England, 1994).
[29] M. S. Longair in *High-energy astrophysics. Vol. 1: Particles, photons and their detection* (Cambridge University Press, Cambridge, England, 1992).
[30] R. Schlickeiser, *Cosmic Ray Astrophysics* (Springer-Verlag, Berlin-Heidelberg, 2002).
[31] L. J. Gleeson and W. I. Axford, Astrophys. J. **154**, 1011 (1968).
[32] O. G. Benvenuto and J. E. Horvath, Mod. Phys. Lett. A **4**, 1085 (1989).
[33] G. A. Medina-Tanco and J. E. Horvath, Astrophys. J. **464**, 354 (1996).